

We thank the referee for his positive appraisal of our manuscript and for the work done to review it. The suggestions of the referee will actually improve the paper.

We address here a first reply to the referee comments before to provide a revised manuscript.

- p. 3 - l. 4: “thalweg” or simply “bottom”?

Here, “bottom” would be more appropriate than “thalweg”.

- p. 9 - l. 9: Is it “Hypothesis” or “Assumptions”?

Some of the “assumptions” made in this subsection are further validated by the results. Thus, they can be considered as “hypothesis”. However, it is true that a part of the assumption cannot be validated with our data: for example the negligible interaction between the sediment classes. Hence, we are agree to change “hypothesis” for “assumption” in this subsection title, and we thanks the referee for this subtlety of the English language.

- p. 11 - l. 24: “regression slope” should be defined or specified, or better at least better linked to what is said elsewhere (I think it is “alpha”?), and p. 11 - l. 25: What is meant by “measured alpha”?

Fig.2 shows the relations obtained from the field measurements between an index concentration sampled close to the river surface and the cross-sectional average concentration measured with a point sampling method. Thus, here the “measured α ” refers to the ratio between index and average concentration (i.e. the total sediment concentration), calculated for each measurement, by contrast with the “predicted α ” calculated with the model from hydraulic parameters (Eq. 15 and 17). For each station, a linear calibration line with a zero intercept was fitted on the measured α values, with a zero intercept (Fig.2). The “regression slope” value fitted on the measured α corresponds to a mean α value for each station and allows comparing the different trends observed on the Fig.2.

In the final reply, this paragraph will be reworded in order to clarify the text.

- p. 12 - l. 28 to - p. 10 - l. 21: That is already a whole lot of interpretation, not only results.

We guess the referee means p. 11, l. 28 to p. 12, l. 21. Yes, this part of the text contains already a lot of interpretations. We believe that the main interest of this part of the paper is to show with observed data that the ratio α between index and average concentration depends on both the basin characteristics and the flow conditions. We can either shorten it, or put it into discussion

- p. 12 - l. 2: Is there a reference for this statement about the delivery of “coarser elements” by the lowland tributaries?

To our knowledge, no reference strictly support the claim that the lowland provides sediments with a coarser grain size than does the central Andean source. This is an assumption partially supported by our grain size data and the following reasoning about the transport capacity (or river competence, i.e. the grain size the river can transport) of the Marañón River, and the main sources of the sediment transported by this river:

The Upper Marañón River mostly drains the Marañón fold and thrust belt in the hollow of the Central Andes, (Pffifner & Gonzales, 2013), with a lithology mainly sedimentary and roughly exposed to the same rainfall regime.

In the lowland, the left bank tributaries, fueled by an equatorial rainfall regime upon the northern part of the basin, supply almost 55% of the Marañón water discharge. These tributaries drain small Andean areas (which are not part of the central Andes), where igneous rocks predominate and with relatively

low erosion rates (Laraque et al., 2009; Armijos et al., 2013) compared to those observed in the central Andes (i.e. for the Ucayali basin, or the Madre de Dios, Beni and Mamore rivers in Bolivia) (Guyot et al., 2007; Armijos et al., 2013; Pepin et al., 2013; Santini et al., 2014; Latrubresse & Restrepo, 2014; Vauchel et al.; 2017, Calvès et al., 2018).

Thus, we deduced that a substantial part of these tributaries fluxes comes from the wide Cenozoic sedimentary basin located between the Marañón River and the Ecuadorian Andes. This large area, partly drained by the Pastaza and Napo Rivers, experiences a neo-tectonics activity (e.g. the uplift of the Mera Megafan) (Baby et al., 2013, Calvès et al., 2018).

If, until now, none long-term survey has been able to quantify these tributaries inputs, the Napo River sediment budget (Laraque et al., 2009; Armijos et al., 2013b) shows that this lowland area could be the main sediment source for the Marañón's Ecuadorian tributaries crossing it.

This secondary source **could** provide sediments with a coarser grain size than the Central Andean source, as the Napo River does (Table 2). In addition, the transport capacity (slope and water level) of the lower Marañón is higher than the Ucayali's one, thus the river can route this material more easily to its outlet.

Moreover, in the lowland, the floodplain incision mechanically increases the sand mass fraction X_s in the suspended load. Implicitly, the PSD mean diameter shifts with X_s , but it does not mean that there is any change in the physical properties (e.g. diameter, density and shape) of the sand fraction. This shift directly affects the ratio α , as the vertical concentration gradient depends on the balance between the turbulence strength and the settling velocity (Eq. (4)).

In contrast, the Ucayali and Huallaga's fluxes routed in the lowland mainly originates from the Central Andes, with a predominant contribution of the Eastern Cordillera slopes and its adjacent Sub Andean Zone (e.g. Aalto et al., 2006; Baby et al., 2009; Kober et al., 2015), where the outcrops are mainly Paleozoic and Mesozoic sedimentary rocks (Pfiffner & Gonzales, 2013). Owing to a monsoon-controlled regime, the rainfall spatial distribution may be roughly considered as pseudo-proportional on the basin. Hence, the composition of the mineralogical convoy of this primary source of sediments may be regarded as relatively stable over time, each lithological domain of the Central Andes contributing in a pseudo-proportional manner. Some discrepancies from this general pattern are however due to the variability in land use, hillslope, regolith thickness, soil erodibility, and others secondary factor.

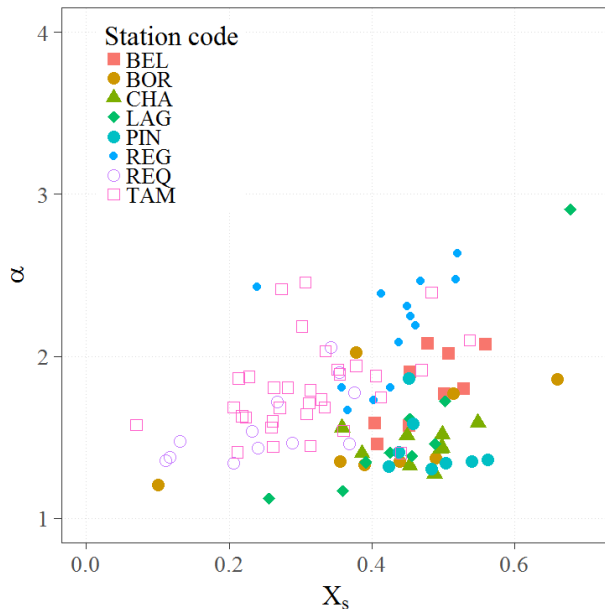
In the floodplain, unlike the Marañón basin, few lateral tributaries come to swell the rivers discharge (Guyot et al., 2007; Armijos et al., 2013; Santini et al., 2014). The nature of the sediment routed through the riverine system depends only of the river transport capacity (weaker than in the Marañón and seasonal) and of the flows back from the floodplain after storage.

- p. 12 - I. 5: Isn't BOR right at the Andean outlet, and therefore not influenced by lowland inputs?

The Upper Marañón River and the Santiago River form the Marañón River at BOR. The Santiago River originates in the Ecuadorian Andes, and crosses a piggyback basin before to reach the Marañón River. This area is considered in the text (roughly) as a lowland area. Conversely, the upper Marañón River originates from the central Andes. Recent concentration measurements made in the upper Marañón River (just before the Andean outlet) have shown that $\alpha = \langle C \rangle / C(h) \cong 1.5$ for this river. This value is consistent with the ratios $\alpha = \langle C \rangle / C(h)$ observed in the other rivers having the Central Andes as a main source of sediments, i.e. the Ucayali and Huallaga rivers, and differs from the ratios α observed in the Napo River and the Marañón River at REG, where the lowland contribution is assumed to explain the high ratios α observed (please report to the argumentation exposed in the previous point).

- p. 12 - l. 7: This is not what I see in Fig. 3... Aren't the axes swapped? And is the color-coding right? The figure and the text sound contradictory, but I might be wrong.

According to referee #1 and #2 reports, Fig.3 is quite difficult to read. We propose the following figure instead, where we can see the increase of $\alpha = \langle C \rangle / C(h)$ with the sand mass fraction X_s . The concentration uncertainty and the shear stress variability during the hydrological cycle explain the dispersion observed in this figure.



New figure 3: Measured $\alpha = \langle C \rangle / C(h)$ vs sand mass fraction X_s . The uncertainty on the concentrations measured and the shear stress variability during the hydrological cycle explain the dispersion observed on the figure.

- p. 12 - l. 14: "increases" with what? Downstream?

Here, we mean that more the particle size is large, more the transport regime may be considered to be capacity-limited, depending only on the available energy to route the sediments.

- p. 12 - l. 27: "mixed-load" should be defined.

"mixed-load" will be defined in the revised manuscript: The mixed-load is a transition mode of transport, where both bedload and suspended load contribute to the total load in similar proportion. The mixed load regime is found when $\sim 1 < P_\phi < 6$.

- p. 12 - l. 28: "random factor" is not clear? Is it meant that this feature appears sort of stochastically?

Here, we propose to reword "random factor" by "uncertainty factor". Indeed, the term "random factor" was poorly chosen to explain why the coarse bed sediments corresponding to the yellow distribution in Fig.4 complicate the prediction and measurement of the concentration profiles.

Bedforms may affect the process of suspension for the coarser fractions of sands because eddies formed at their leeward side, can swiftly uplift large amounts of this sediments in the water column (fluid burst). Along with the water height and the turbulence structures expansion, the suspension of these coarse sediments becomes rather stochastic than uniform, as their grain size make them very sensitive to the velocity fluctuations, which are stochastic. Thus, their presence is non-permanent and

heterogeneous across the section (and often associated to the movable bed phenomenon affecting the ADCP measurements when none GPS is coupled with this instrument).

Hence, the concentration of this sand fraction is very difficult to measure: at least, such measurement would require a long integration time during the sampling operation to obtain a representative estimate.

Moreover, the suspension of this coarse material may be fundamentally different to the suspension described with a classical diffusion approach (i.e. when considering uniform conditions). Indeed, the stochastic and ephemeral inputs of coarse bed material in the water column is not addressed by the classical suspension theory (inferred from the Prandtl mixing length approximation), which considers time-averaged concentrations and neglects the fluctuation terms (see also the section 4.2, P.17, l.25 to 27).

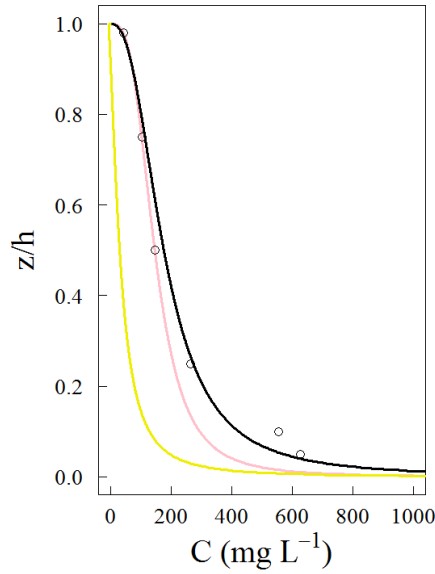
However, such process is rather limited to the first heights of the water column and concern a small fraction of the total load in suspension (when a long enough timescale is considered, which is usually the case for basic sediment load assessments in large rivers). This is why it is rather an “uncertainty factor” than a “random factor”.

- p. 12 - l. 29-30: Is this link clearly established, actually?

This follows up the previous point. During the fitting procedure of suspension models on the observed concentration profiles, we noticed that some profiles were more disturbed (i.e. more dispersed) on the lower half of the water column for high flow conditions than for normal flow conditions. We related these concentration fluctuations to a more important influence of the coarse bed sands uplifted in suspension (yellow distribution in Fig.4) on the measured concentration.

The following figure show how the coarse sand fraction can affect the Rouse number value fitted on concentration profiles. The black circles are observed sand concentrations over depth on a sampled vertical at TAM. At this vertical, a movable bed phenomenon was detected during the ADCP measurement. The continue line in black correspond to a Rousean profile fitted on the concentrations measured. A second Rousean profile was fitted on the three first points of the water depth (pink line, which would correspond to the pink distribution in Fig. 4a). The yellow profile results from the difference between the two previous ones. Assuming that no coarse sediments are present in the upper part of the flow, the yellow profile would correspond to the mixed-load represented by the yellow distribution in Fig. 4a.

In this example, the mixed-load weight moderately on the Rouse number fitted on the sand concentration profile (here, the Rouse number for the pink profile is equal to 0.33, and equal to 0.4 for the black profile). However, when considering a mean concentration profile for the whole cross-section, the mixed-load influence decrease, as its presence is heterogeneous across the section.



- p. 13 - l. 25-26: Which “result” exactly are we talking about here? The P-values themselves or their low variability. Or the fact that they were averaged per site?

We guess the referee means p. 13, l. 15-16. The low variability of the Rouse numbers fitted on the concentration profiles indicates there is a kind of dynamic equilibrium between the sediment settling velocity and the shear stress under nominal flow conditions, although some extreme Rouse number values were measured during severe drought events at the lowland stations.

- p. 14 - l. 22: Which “zone”?

This is the flow zone near the water surface ($\alpha_s(h, P_s)$). We will reword the sentence in the revised manuscript in order to clarify the text.

- p. 16 - l. 29: Where are the numerical values in the equation from?

The original Rose and Thorne (2001) law $\beta_\phi = 3.1 \exp\left(-0.17 \frac{u_*}{w_\phi}\right)$ is an empirical function based upon a regression analysis on measured concentration profiles. The factor 3.1 of Eq. 19 is coming from this law.

In the present work, the following modification of the Rose and Thorne (2001) law is proposed:

$$\beta_\phi = 3.1 \exp\left(-0.19 \frac{u_* \left(\frac{h}{d_s}\right)^{0.6}}{1000 \times w_\phi}\right) + 0.16$$

where the numerical values of Eq. 19 were fitted to obtain the best agreement between the β_ϕ inferred from the measured concentration profiles (Table 2) and the β_ϕ predicted by Eq.19.

The following correction of the $\left(\frac{u_*}{w_\phi}\right)$ ratio allows reducing the discrepancy observed in (Fig. 8a) between the Rose and Thorne law and the observed β_ϕ values:

$$\left(\frac{u_*}{w_\phi}\right)_{corrected} = \frac{0.19 \left(\frac{h}{d_s}\right)^{0.6}}{0.17 \cdot 1000} \left(\frac{u_*}{w_\phi}\right)$$

The original Rose and Thorne law tends to zero for low values of the ratio $\left(\frac{u_*}{w_\phi}\right)$ (Fig. 8a). Adding a value of 0.16 allows to take into account the β_f for the fine sediments in the modified law (Fig. 8b).

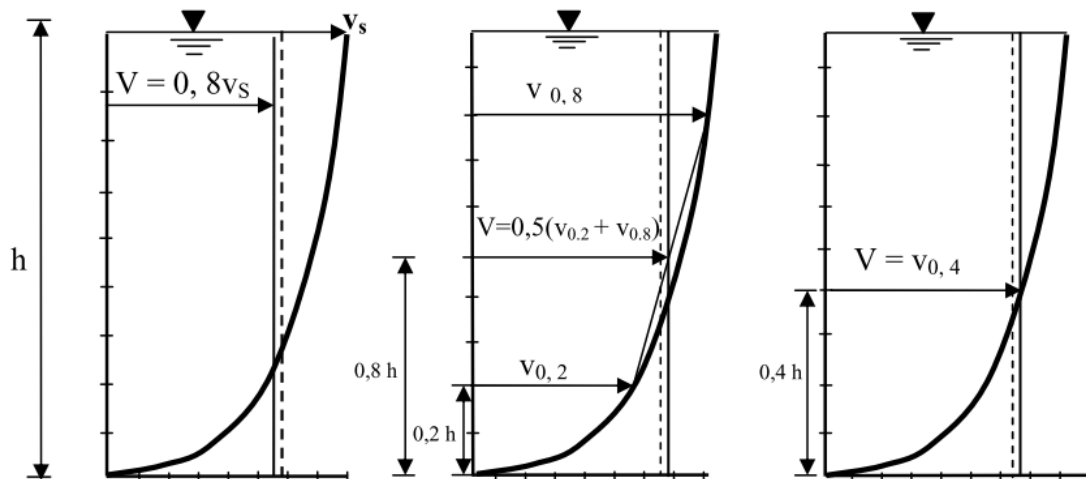
- p. 19 - I. 9: Where does this relationship between “<u>” and “h” come from?

When the stream's velocity profile is logarithmic in nature $\left(u(z) = \frac{u_*}{\kappa} \ln\left(\frac{z}{z_0}\right)\right)$, it can be shown that the depth-integrated velocity $\langle u \rangle$ is equal to: $\langle u \rangle \cong \frac{h}{e} \cong 0.37h$:

$$\int_{z_0}^h \frac{u_*}{\kappa} \ln\left(\frac{z}{z_0}\right) dz \cong \frac{u_*}{\kappa} (\ln(h) - 1) - \frac{u_*}{\kappa} \ln(z_0) \cong \frac{u_*}{\kappa} \ln\left(\frac{h}{e}\right) = u\left(\frac{h}{e}\right), \text{ with } \ln(e) = 1 \text{ and } h \gg z_0$$

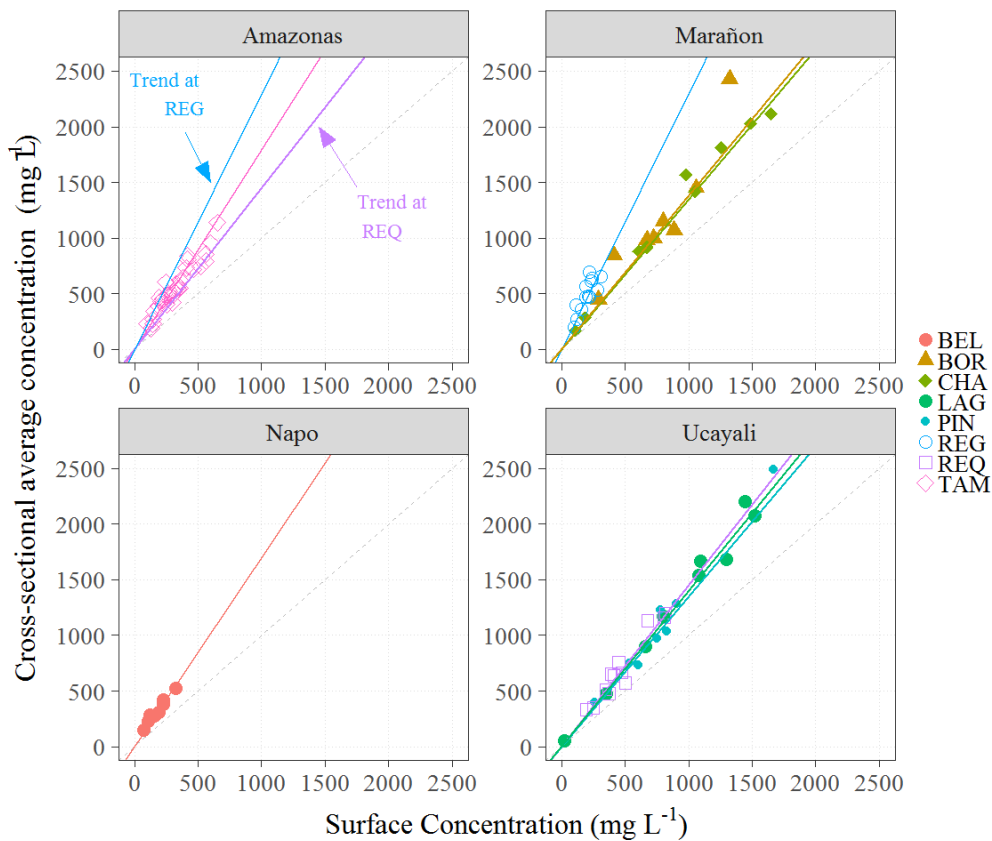
It is a result well known by the hydrologist measuring river discharges with a classic current-meter. Other points of interest exist on the velocity profile: Prony first shown that usually $\langle u \rangle \cong u(0.8h - 0.9h)$. The USGS recommends to deploy a two points method: $\langle u \rangle \cong \frac{1}{2}(u(0.8h) + u(0.2h))$. This method could be also coupled with Eq. 21 in order to define a protocol for concentration measurement.

When the velocity profile is not logarithmic (which is often the case in small streams with high Froude numbers), a three-point method can also be deployed (0.8h, 0.4h, 0.2h).



- Figure 2: It took me a while to understand what the blue and purple lines are in the upper-left panel
 - it would be better to clearly indicate what they are within the panel.

Please find below a new figure 2 with a short text in the upper left panel:



- What the x-axis represents is a bit mysterious, as I did not see any explanation in the text. I guess this is because this is a non-dimensional number that is expected to be the same at all locations and in all hydrological conditions?

We guess it is the x-axis of Fig. 5 and not Fig. 2? If it is Fig. 5, yes, it is a non-dimensional number, and the diffusivity profile is expected to follow the theoretical models (Camenen & Larson, Rouse, Van Rijn or Zagustin) at all locations and in all hydrological conditions.

- Figure 7, caption: What is meant by “observed” and “measured” values here?

For each site, mean α_f and α_s were computed according to Eq. 17 with the mean parameters given in table 2. Then, “predicted α ” were calculated from Eq. 15 ($\alpha = X_f \alpha_f + X_s \alpha_s$), by considering the mean X_f and X_s values also given in table 2 and calculated from the concentration measurements. Finally, the “predicted α ” are compared in Fig.7 with the “observed α ”, i.e. the mean ratios between index and average total concentration, measured at each site. The “observed α ” corresponds to the slope of the regression lines in Fig. 2.

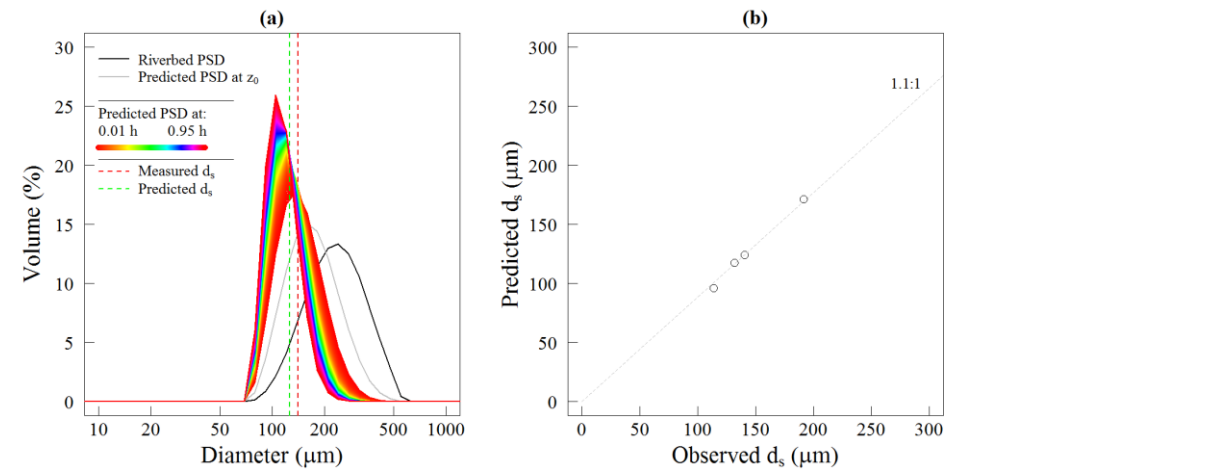
Maybe we could change “observed α ” for “measured α ” both in the ms and in the figure 7?

- Figure 10: What about the other stations than those shown in panel (b), why aren't they represented? And it would make more sense to me to plot simply “predicted” vs. “measured” (i.e. without the 1.1-factor) and then to plot the 1:1, and/or 1.1:1 line – at least because in this case the caption is wrong, strictly speaking.

Samples for the characterization of the bed material PSD were collected only in four sites: BEL (2 PSD), REQ (1 PSD), REG (1 PSD) and TAM (2 PSD). Please note that for TAM and BEL, only the average diameter of the two PSD measured is plotted (However, we could plot all the measurements if necessary). There is no PSD measurements for the bed material at BOR, LAG, PIN and CHA. We will add

some words in the revised ms about the collection of bed material in the “material and methods” section.

Please find below the new figure 10 with the modification asked:



Technical corrections

- p. 12 - l. 21 (also p. 15 - l. 3): “valid” -> “validate”.
- p. 14 - l. 17: “is” -> “are”.
- p. 17 - l. 5: “in” -> “at”.
- p. 20 - l. 5: Something is missing between “can” and “more”.
- p. 20 - l. 7: “the ratio of” -> “the ratio between”?
- p. 20 - l. 11: “ad” -> “and”.
- Figure 2, caption: “staked” -> “stacked”.

Many thanks for the technical corrections; we will incorporate them in the revised ms.

Sincerely,

William Santini

References:

Aalto, R., Dunne, T., Guyot, J. L.: Geomorphic Controls on Andean Denudation Rates, *The Journal of Geology* 114(1), 85-99, doi:10.1086/498101, 2006.

Armijos, E., Laraque, A., Barba, S., Bourrel, L., Ceron, C., Lagane, C., Magat, P., Moquet, J. S., Pombosa, R., Sondag, F., Vauchel, P., Vera, A., Guyot, J. L.: Yields of suspended sediment and dissolved solids from the Andean basins of Ecuador, *Hydrological Sciences Journal*, 58(7), 1478-1494, doi:10.1080/02626667.2013.826359, 2013b.

Baby, P., Guyot, J. L.: Tectonic control of erosion and sedimentation in the Amazon Basin of Bolivia, *Hydrological Processes*, 23(22), 3225-3229, doi:10.1002/hyp, 2009.

Baby, P., Rivadeneira, M., Barragan, R., Christophoul, F.: Thick-skinned tectonics in the Oriente foreland basin of Ecuador, *Geological Society, London, Special Publications* 377(1), 59-76, doi:10.1144/SP377.1, 2013.

- Calvès, G., Calderon, Y., Hurtado Enriquez, C., Brusset, S., Santini, W., Baby, P.: Mass Balance of Cenozoic Andes-Amazon Source to Sink System, Marañon Basin, Peru, *Geosciences* 8(5), 167, doi:10.3390/geosciences8050167, 2018.
- Kober, F., Zeilinger, G., Hippe, K., Marc, O., Lenzioch, T., Grischott, R., Christl, M., Kubik, P., Zola, R.: Tectonophysics Tectonic and lithological controls on denudation rates in the central Bolivian Andes, *Tectonophysics* 657, 230-244, doi:10.1016/j.tecto.2015.06.037, 2015.
- Latrubesse, E. M., Restrepo, J. D.: Sediment yield along the Andes: continental budget, regional variations, and comparisons with other basins from orogenic mountain belts, *Geomorphology* 216, 225-233, doi:10.1016/j.geomorph.2014.04.007, 2014.
- Pepin, E., Guyot, J. L., Armijos, E., Bazan, H., Fraizy, P., Moquet, J. S., Noriega, L., Lavado, W., Pombosa, R., Vauchel, P.: Climatic control on eastern Andean denudation rates (Central Cordillera from Ecuador to Bolivia), *Journal of South American Earth Sciences*, 44, 85-93, doi:10.1016/j.jsames.2012.12.010, 2013.
- Pfiffner, A. O., Gonzalez, L.: Mesozoic–Cenozoic Evolution of the Western Margin of South America: Case Study of the Peruvian Andes, *Geosciences* 3(2), 262–310, doi:10.3390/geosciences3020262, 2013.